

# Applying new tools to old problems—experimental studies of resonances in $^{12}\text{C}$

O S Kirsebom, H O U Fynbo, A M Howard and K L Laursen

Department of Physics and Astronomy, Aarhus University, 8000 Aarhus C, Denmark

E-mail: [oliskir@phys.au.dk](mailto:oliskir@phys.au.dk)

**Abstract.** We report preliminary results from an experimental study of the  $p + ^{11}\text{B}$  reaction at beam energies of 2.00 MeV, 2.63 MeV and 3.12 MeV, corresponding to three known  $0^+$ ,  $2^+$  and  $3^-$  resonances in  $^{12}\text{C}$  at excitation energies of 17.79 MeV, 18.38 MeV and 18.81 MeV. The resonances have small  $\gamma$ -decay branches to lower-lying resonances of the order of  $10^{-6}$ – $10^{-5}$ . By detecting the three outgoing  $\alpha$  particles in coincidence and measuring their momenta, we obtain complete kinematics information. From the combined energy of the  $\alpha$  particles we determine the energy of the  $\gamma$  transition. In this way, we identify two previously observed transitions,  $(0^+, 17.79) \rightarrow (1^+, 12.71)$  and  $(3^-, 18.38) \rightarrow (3^-, 9.64)$ , and one new transition,  $(2^+, 18.81) \rightarrow (1^+, 12.71)$ . The results demonstrate the usefulness of  $\gamma$  decay as a probe of the low-lying resonance spectrum of  $^{12}\text{C}$  in the search for new broad (cluster) resonances.

## 1. Introduction

### 1.1. Turning a disadvantage into an advantage

The famous Dutch footballer Johan Cruyff supposedly coined the phrase “every disadvantage has its advantage”. In nuclear-reaction experiments, high multiplicity used to be considered a disadvantage because it was very difficult to detect more than two particles in coincidence. Consequently, only *partial* kinematic information was obtained, which made it difficult to single out the reaction channels of interest because a clear signature was missing (such as a peak in the sum-energy spectrum). Within the last two decades, however, multi-particle coincidence measurements have become feasible thanks to the advent of compact arrays of segmented silicon detectors, and with *complete* kinematic information now available, the disadvantage of having many particles in the final state turns into an advantage: Not only can we make a clean selection, but one that is *cleaner* than for low-multiplicity channels because high-multiplicity channels are comparatively rarer. High-multiplicity studies are, of course, closely connected to the topic of this conference, as clustering phenomena in nuclei manifest themselves most strongly at excitation energies close to or somewhat above particle-decay thresholds.

### 1.2. Putting two old accelerators back into use

Aarhus University has two Van de Graaff accelerators at its disposal, which have been in operation since the 1960s. The accelerators have been used primarily for material analysis and student exercises, but recently we have started using them for nuclear-physics experiments. The smaller accelerator goes up to 400 kV, the larger to about 4 MV (nominally 5 MV). The



results presented here were obtained at the 5 MV accelerator. Results obtained at the 400 kV accelerator will be presented by K. L. Laursen in a separate contribution.

We use a compact array of double-sided silicon strip detectors (DSSDs) to revisit “well-known” nuclear reactions induced by few-MeV beams of  $^1\text{H}$ ,  $^3\text{He}$  or  $^4\text{He}$  on light-element targets such as Li, Be, B, C and N. We focus on reactions with high  $Q$  value leading to final states with high multiplicity, examples of which being  $^6\text{Li}(^3\text{He}, p2\alpha)$  and  $^{10}\text{B}(^3\text{He}, p3\alpha)$ . The combination of high granularity and large solid-angle coverage allows us to measure multi-particle coincidences with high resolution and high efficiency. Having complete kinematic information, we are able to improve on previous studies both quantitatively and qualitatively. In particular, we are able to extract new and valuable information on resonances in light nuclei of relevance both to nuclear astrophysics and nuclear structure. Since the demand for the two Van de Graaff accelerators is low, we are able to run for extended periods of time (several weeks), making it possible to accumulate enough statistics to study rare decay modes.

## 2. First experiment: $p + ^{11}\text{B}$

### 2.1. Motivation

In recent years, the topic of  $\alpha$  clustering in  $^{12}\text{C}$  has generated numerous papers, both theoretical and experimental, and at the present conference, a considerable number of contributions have been devoted to the topic. Arguably the most significant step forward on the experimental side has been the identification of a new  $2^+$  resonance at an excitation energy of 10.1 MeV [1]. The properties of the resonance remain to be pinned down. Whether it can be viewed as a rotational excitation of the Hoyle state is at present not clear<sup>1</sup>. Recent experiments have uncovered evidence of additional new resonances<sup>2</sup>, but the search is challenging. The “easy” (relatively narrow) resonances have all been found, leaving only the “tough” (broad) ones. A more complete experimental picture of the resonance spectrum of  $^{12}\text{C}$  is necessary to advance the theoretical understanding of  $\alpha$  clustering in  $^{12}\text{C}$ . It is also a necessary prerequisite for an accurate determination of the stellar triple- $\alpha$  rate at elevated temperatures [2]. Clearly, a complementary approach is necessary. No single reaction or decay will give us the full answer.

### 2.2. Experimental approach

The reaction  $p + ^{11}\text{B}$  has been used by many experimenters to study resonances in  $^{12}\text{C}$  above the proton-decay threshold. Many experimenters have studied the breakup into three  $\alpha$  particles. Hanna *et al.* have studied the  $\gamma$  decay to lower-lying states [3]. We have collected complete-kinematics data on both decay mechanisms. Here, we present preliminary results on the  $\gamma$ -decay mechanism. The full results (on both decay mechanisms) will be presented in forthcoming papers. Hanna *et al.* were mainly interested in the structure of the initially populated state in  $^{12}\text{C}$ . In contrast, we are mainly interested in the state populated in the subsequent  $\gamma$  decay. A schematic illustration is given in Figure 1.

Like the  $\beta$  decays of  $^{12}\text{B}$  and  $^{12}\text{N}$ ,  $\gamma$  decay is a highly *selective* probe of the low-lying resonance spectrum in  $^{12}\text{C}$  in the sense that the decay is governed by selection rules that strongly favour the population of states with certain spin-parities [4]. In  $\beta$  decay the spin and parity of the initial state, and hence the selection rules, are fixed. In  $\gamma$  decay there is no similar restriction as we can use the  $p + ^{11}\text{B}$  reaction (or another suitable reaction) to populate states with spin-parities of our preference (to the extent that such states exist). Thus,  $\gamma$  decay constitutes not only a highly selective but also an *adjustable* probe. Its main disadvantage is the low branching ratio for  $\gamma$  decay, typically of the order of  $10^{-6}$ – $10^{-5}$ . The spin-parities that can be reached via E1,

<sup>1</sup> See the contribution of Garrido.

<sup>2</sup> See the contributions of Itoh, Kokalova, Gai, Laursen and Marín-Lámbarri.

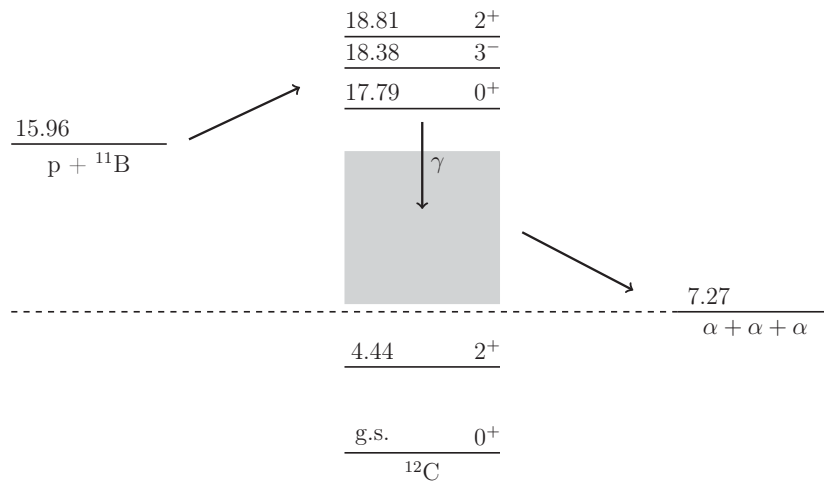


**Figure 1.** Schematic illustration of experimental approach: The reaction  $p + {}^{11}\text{B}$  is used to populate selected resonances in  ${}^{12}\text{C}$  that  $\gamma$  decay to lower-lying resonances, which subsequently break up into three  $\alpha$  particles. The  $\alpha$  particles are detected and the occurrence of a  $\gamma$  transition is deduced from the missing energy.

**Table 1.** Spin-parities that can be reached via E1, M1 and E2 transitions. The initial states are labeled by their excitation energy in MeV and spin-parity.

$E\ell/M\ell$	17.79, $0^+$	18.38, $3^-$	18.81, $2^+$
E1	$1^-$	$2^+, 3^+, 4^+$	$1^-, 2^-, 3^-$
M1	$1^+$	$2^-, 3^-, 4^-$	$1^+, 2^+, 3^+$
E2	$1^+, 2^+$	$1^-, \dots, 5^-$	$0^+, \dots, 4^+$

M1 and E2 transitions in the present experiment are listed in Table 1. Isospin selection rules provide additional selectivity.

### 2.3. Setup and data analysis

The detector setup is shown in Figure 2. It consists of two  $24 \times 32$  annular DSSDs, which cover the forward-most angles ( $16^\circ$ – $42^\circ$ ) and the backward-most angles ( $142^\circ$ – $166^\circ$ ), and two  $16 \times 16$  square DSSDs, which cover the intermediate angles ( $53^\circ$ – $127^\circ$ ). The annular DSSDs are 1 mm and  $64 \mu\text{m}$  thick, respectively, and the square DSSDs are both  $60 \mu\text{m}$  thick. The detectors view the target from a distance of 4 cm and provide a solid-angle coverage of 40% of  $4\pi$ , giving in a triple- $\alpha$  coincidence detection efficiency of the order of 6%. Both ADC (energy) and TDC (time) information is recorded. For the present experiment, the target was  $7 \mu\text{g}/\text{cm}^2$  natural boron on a  $4 \mu\text{g}/\text{cm}^2$  carbon backing. The typical beam intensity was 0.3 nA as measured in a Faraday cup downstream of the detector setup. The beam diameter was less than 3 mm at the target site. Measurements were performed at beam energies of 2.00 MeV, 2.63 MeV and 3.12 MeV, corresponding to three known  $T = 1$  resonances with spin-parities of  $0^+$ ,  $2^+$  and  $3^-$  and excitation energies of 17.79 MeV, 18.38 MeV and 18.81 MeV. The duration of the measurements were 41 h, 30 h and 32 h, respectively.

The occurrence of a  $\gamma$  transition can be inferred from the missing energy carried away by the

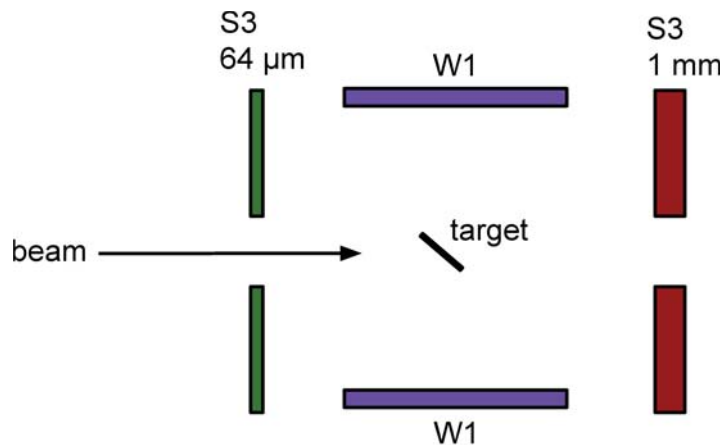


**Figure 2.** Schematic illustration of the detector setup (top view). The beam comes in from the left. The target is surrounded by four DSSDs in a rectangular configuration. Two annular DSSDs (S3) cover forward and backward angles and two square DSSDs (W1) cover intermediate angles.

$\gamma$  ray. The  $\gamma$  ray itself is not detected. As demonstrated in a previous study [5], the technique is particularly useful to identify  $\gamma$  transitions to broad states. The present setup does not allow us to distinguish between different types of ions. At the beam energies used in the present study, the only energetically allowed three-body final state in the  $p + {}^{11}\text{B}$  reaction is  $\alpha + \alpha + \alpha$ . However, reactions on  ${}^{10}\text{B}$  can give  $\alpha + \alpha + {}^3\text{He}$ . Random coincidences between, say, an elastically scattered proton and two  $\alpha$  particles can also give a triple coincidence that “mimics” a triple- $\alpha$  event. The background due to such false triple- $\alpha$  events is reduced by imposing a number of cuts in the data analysis: TDC information is used to reduce the background due to random coincidences by a factor of  $\sim 40$ . Further reduction is achieved by placing an anti-gate on the kinematic curve of elastically scattered protons and the kinematic curve of  $\alpha$  particles from the reaction  ${}^{10}\text{B}(p, \alpha){}^7\text{Be}$ . Finally, we require the total momentum to be conserved (the momentum carried away by the  $\gamma$  ray is negligible).

### 3. Preliminary results

In our data, we find clear evidence of the following  $\gamma$ -ray transitions,

- (i)  $0^+, 17.79 \rightarrow 1^+, 12.71$
- (ii)  $3^-, 18.38 \rightarrow 3^-, 9.64$
- (iii)  $2^+, 18.81 \rightarrow 1^+, 12.71$

We also find tentative evidence of other transitions, but a careful analysis of the background is necessary before firm conclusions will be drawn. Transitions (i) and (ii) were observed previously by Hanna *et al.* [3] whereas transition (iii) appears not to have been observed previously. Monte Carlo simulations will be performed in the near future to determine the detection efficiency of the setup. This will enable us to extract branching ratios.

The complete-kinematics data collected on the  $2^+$  resonance are shown in Figures 3 (a) and (b). Figure (a) shows the momentum deficit, defined as

$$\Delta p = \left| \vec{p}_p - \sum_{i=1,2,3} \vec{p}_{\alpha_i} \right| \quad (1)$$

where  $\vec{p}_p$  is the momentum of the beam and  $\vec{p}_{\alpha_i}$  are the  $\alpha$ -particle momenta, versus the excitation energy in  $^{12}\text{C}$ , determined as

$$E_x = S_{3\alpha} - \frac{1}{12}E_p + \sum_{i=1,2,3} E_{\alpha_i} \quad (2)$$

where  $S_{3\alpha} = 7.27$  MeV is the triple- $\alpha$  threshold energy in  $^{12}\text{C}$ ,  $E_p$  is the beam energy and  $E_{\alpha_i}$  are the  $\alpha$ -particle energies. The momenta and the energies are all measured in the laboratory frame. TDC information has been used to reduce the background due to random coincidences. Further reduction has been achieved by placing an anti-gate on the kinematic curve of elastically scattered protons and the kinematic curve of  $\alpha$  particles from the reaction  $^{10}\text{B}(p, \alpha)^7\text{Be}$ . By imposing the additional requirement  $\Delta p < 55$  MeV/c (dashed line), we obtained the excitation-energy spectrum shown in Figure (b). The main peak (E) corresponds to the ordinary decay mechanism, *i.e.*, breakup into three  $\alpha$  particles without a preceding  $\gamma$  transition; (C) is the previously unobserved  $\gamma$  transition to the 12.71 MeV state; (B) and (D) are potential candidates for new  $\gamma$  transitions; finally, (A) corresponds to  $\alpha + \alpha + ^3\text{He}$  events from reactions on  $^{10}\text{B}$ . By gating on the narrow ground state of  $^8\text{Be}$  in the  $\alpha$ - $\alpha$  relative-energy spectrum, it is possible to single out the breakups that proceed via the ground state of  $^8\text{Be}$ . By considering only these breakups, one obtains the gray-shaded spectrum. Note that peak (C) is absent in the gray-shaded spectrum. This is consistent with the proposed interpretation, as parity conservation forbids the breakup of unnatural-parity states via the  $0^+$  ground state of  $^8\text{Be}$ .

#### 4. Summary and outlook

At Aarhus University in Denmark we have built a new facility to study nuclear reactions induced by few-MeV beams of  $^1\text{H}$ ,  $^3\text{He}$  or  $^4\text{He}$  on light-element targets such as Li, Be, B, C and N. The detection system consists of a compact arrangement of segmented silicon detectors, allowing many-particle final states to be studied in complete kinematics. Here, we have reported preliminary results from the first experiment at the new facility. We have studied the decay of three selected resonances in  $^{12}\text{C}$  populated via  $p + ^{11}\text{B}$ . The resonances have small  $\gamma$ -decay branches ( $10^{-6}$ – $10^{-5}$ ) to lower-lying resonances which subsequently break up into three  $\alpha$  particles. We have determined the energy of the  $\gamma$  transition from the combined energy of the  $\alpha$  particles. In this way, we have identified two previously observed transitions,  $(0^+, 17.79) \rightarrow (1^+, 12.71)$  and  $(3^-, 18.38) \rightarrow (3^-, 9.64)$ , and one new transition,  $(2^+, 18.81) \rightarrow (1^+, 12.71)$ . We find tentative evidence for additional transitions, but further analysis is required to fully understand the background. Simulations will be performed in the near future to determine the detection efficiency of the setup. This will allow us to extract branching ratios. We are in the process of improving the setup. Important goals include improving the time resolution and acquiring an isotope enriched  $^{11}\text{B}$  target.

#### Acknowledgments

We acknowledge financial support from the European Research Council under the ERC starting grant LOBENA, No. 307447.

#### References

- [1] Zimmerman W R, *et al.* 2013 *Phys. Rev. Lett.* **110** 152502
- [2] Fynbo H O U, *et al.* 2005 *Nature* **433** 136–9
- [3] Hanna S S, Feldman W, Suffert M and Kurath D 1982 *Phys. Rev. C* **25** 1179–86
- [4] Hyldegaard S, *et al.* 2010 *Phys. Rev. C* **81** 024303
- [5] Kirsebom O S, *et al.* 2009 *Phys. Lett. B* **680** 44–9

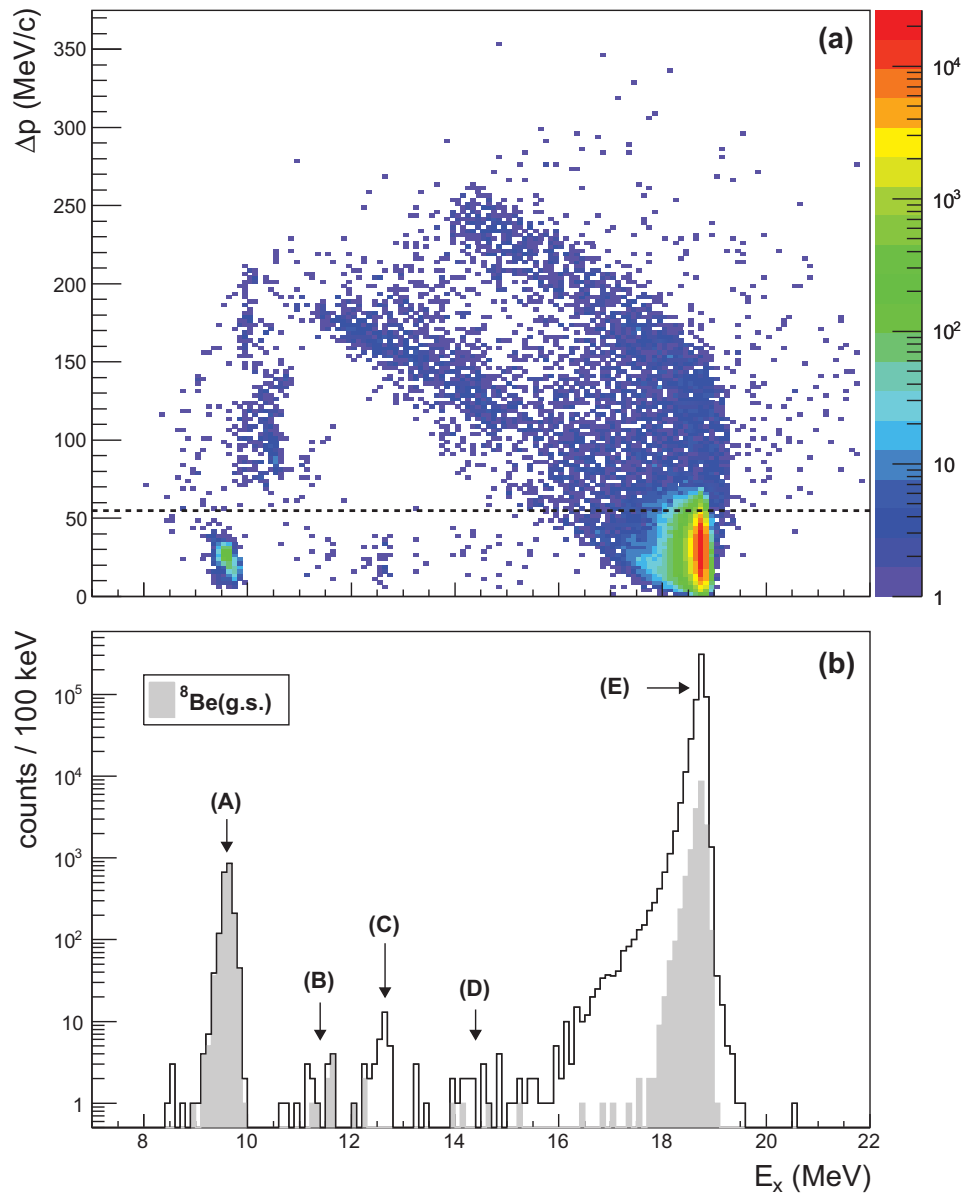


**Figure 3.** Complete-kinematics data collected for the  $2^+$ , 18.81 MeV state. Figure (a) shows the momentum deficit, cf. Eq. (1), versus the excitation energy, cf. Eq. (2). TDC information and kinematic cuts have been used to reduce the background due to random coincidences. Events below the dashed line fulfil momentum conservation. Figure (b) shows the excitation-energy spectrum obtained by considering only events below the dashed line. The interpretation of the five peaks (A)–(E) is discussed in the text. The gray-shaded area is the spectrum obtained by including only decays proceeding via the ground state of  $^8\text{Be}$ .